35th Annual International Conference of the IEEE EMBS
Osaka, Japan, 3 - 7 July, 2013

Evaluating Epicardial Mapping Electrogram by the Method of Dominant Frequency and Lorenz Plot

Liqian Sun, Yanlei Wang, Cuiwei Yang*, Ying Chen, Zhong Wu, Jianguo Yu

Abstract—**The methods of dominant frequency and Lorenz plot are used in this study to evaluate the activation rate and the activation rate variability of cardiac signals during atrial fibrillation. An epicardial mapping system was applied to acquire the atrial electrogram of mongrel dogs. The dominant frequency and Lorenz plot of each signal from various myocardial regions of the atria were analyzed. Our results show that both a frequency gradient and a variability gradient exist in the atria and the roots of pulmonary veins. The dominant frequencies of the anterior atria are higher than the posterior ones and the activation variability of both atria was higher than those of the pulmonary veins. A combination of these two methods may provide a more comprehensive understanding of the electrophysiology mechanism associated with atrial fibrillation.**

I. Introduction

To date, the electrophysiological mechanism of atrial fibrillation (AF) has not been clearly elucidated. The widely accepted multiple-wavelet hypothesis of AF postulates that AF is sustained by numerous coexisting wave fronts of electrical activity that propagate randomly throughout the fibrillating atria [1, 2]. In recent years, dominant frequency (DF) analysis has become an important approach to estimate activation rate of AF signals [3-5]. Certain regions of the atria have been demonstrated to have higher activation rate than other regions, suggesting that these areas may be the drivers that maintain AF and could be the targets of ablation therapy [6-9]. However, DF seems to lose the information about the variability of activation rate for multi-rhythm signals. As a conventional method to evaluate heart rate variability (HRV), Lorenz plot (LP) can just make up for the shortfall [10].

In this study, DF was used to evaluate the activation rate of atrial electrogram (AEG) while LP was used to analyze the variability of activation rate of AEG. To evaluate the variability of activation rate more digitally, we proposed a method using evaluation index based on LP. The aim of this study was to evaluate the activation rate and the variability of activation rate of AEG in various parts of the atria and the roots of pulmonary veins (PV) underlying AF.

This work was supported by the National Natural Science Foundation of China (61071004, 60701002).

Liqian Sun, Yanlei Wang and Jianguo Yu are with the Department of Electronic Engineering, Fudan University, Shanghai 200433, China. (E-mail: Liqian_sun@hotmail.com, king.bryan@yahoo.cn).

*Cuiwei Yang is with the Department of Electronic Engineering, the Center for Intelligent Medical Electronics (CIME) within the School of Information Science and Technology, Fudan University, Shanghai 200433, China. (Corresponding author, phone & fax: +8621-65643709; e-mail: yangcw@fudan.edu.cn).

Ying Chen is with the Department of Electronic Science and Engineering, Nanjing University, Nanjing, China.

Zhong Wu is with the Department of Thoracic and Cardiovascular Surgery, the Affiliated Drum Tower Hospital of Nanjing University Medical School, China.

II. Methods

A. Fibrillation and Mapping

Eight mongrel dogs (weight 13.4 ± 2.9 kg) were studied in vivo. AF was induced by rapid pacing (>1000 bpm) of the left atrial appendage (LAA) or the right atrial appendage (RAA) of the canine heart with an intravenous injection of acetylcholine. 128 unipolar electrodes were placed on eight flexible patches. All patches were attached to the epicardial surface of both the atria and the roots of PVs; their distribution is shown in Fig.1. The horizontal and vertical spacing between the electrodes on different patches are as follows: A: 3.5 mm, 3.5mm; B: 3.5 mm, 3.5mm; C': 4mm, 4mm; C: 4 mm, 4mm; D1: 3 mm, 2 mm; D2: 3 mm, 2 mm; D3: 3 mm, 2 mm; D4: 3 mm, 2 mm. All of these electrodes were connected to the epicardial mapping system (model: FDEMS-2) our lab has developed [11]. AEG were filtered between 3.5-600 Hz, and the sampling frequency was 2 kHz.

B. Pre-processing and Characterization

Our hardware system conducted the signal conditioning work, which included amplifying and filtering. Software pre-processing mainly solved the problem of the ventricular artefacts (mainly due to problems of electrode contact). A least mean square (LMS) adaptive filter with noise canceller model was introduced [12, 13]. We employed the reference signals from the apex of the heart (located in the left ventricle) as input signals to our adaptive filter, while contaminated AEG as additional input signals. Consequently, the error signal of the filter provided an optimum estimate of the desired AEG.

Activation time was defined as the time corresponding to the apex of activation waveform. In this study, a method

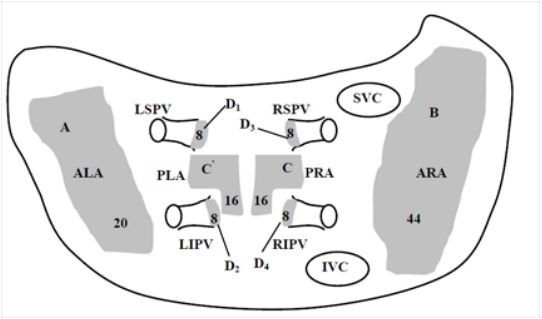

Figure 1. An atrial epicardial mapping schematic diagram. A: anterior left atrium (ALA), B: anterior right atrium (ARA), C': posterior left atrium (PLA), C: posterior right atrium (PRA), D1: left superior PV (LSPV), D2: left inferior PV (LIPV), D3: right superior PV (RSPV), D4: right inferior PV (RIPV), superior vena cava (SVC), interior vena cava (IVC). The areas shaded in gray represented the mapping regions. The numbers in the shaded areas represented the numbers of unipolar electrodes in the regions.

proposed by JiaPu Pan was used to characterize the activation times of the AEG [14].

C. Dominant Frequency

The method of DF was used to estimate the activation rate during AF [5-9]. The DF can be denoted on the magnitude spectrum as the frequency with the highest peak. For local electrograms, recordings always have a sharp biphasic waveform corresponding to rapid depolarization; this morphology prevents a single sinusoid with a frequency equal to the activation rate from "fitting" the signal. Thus, band pass filtering (at 40-250 Hz) steps were used for our AEG before Fourier transform [15, 16].

D. Lorenz Plot

Conventionally, LP was generated for ECG RR intervals, which plotted the nth ECG RR interval on the horizontal axis, and the n+1th ECG RR interval on the vertical axis. In this study, ECG RR intervals were replaced with AEG activation intervals.

Conventional indexes based on LP including long axis, short axis and their ratio have a poor anti-jamming ability of occasional arrhythmia [10, 17]. The nearly circular LP distribution of arrhythmia ECG has introduced the analysis of the correlation between the radius size of the circle and the HRV, which has been proved with academic logic [18-20]. In our study, radius size normalized by average activation interval was used as an evaluating index to calculate the activation variability of AEG. As shown in Fig.2, the steps were as follows: 1) Calculate the average horizontal and vertical axis values and denote it as the centre of LP distribution, denoted as A($\bar{x}, \bar{y}$), in which, $\bar{x} = \sum_i x_i / N$, $\bar{y} = \sum_i y_i / N$, N was the total number of points in the LP; 2) Calculate the distance from each point in the LP to the centre and get the average distance, denoted as $\bar{d}$, in which, $\bar{d} = \sum_i d_i / N$; 3) $\bar{d}$ normalized with the average activation interval ($\overline{AI}$) worked out the final index, termed equivalent radius (ER = $\bar{d} / \overline{AI}$).

III. Results

Sustained AF was induced in live canine hearts with the method mentioned above. For each episode (20 seconds long), AEG from 8 patches were analyzed and compared to demonstrate the DF and ER distribution of various parts in atria during AF. Altogether, 72 episodes of AF were analyzed from 8 experiments. Rank sum test was used to estimate the p-values.

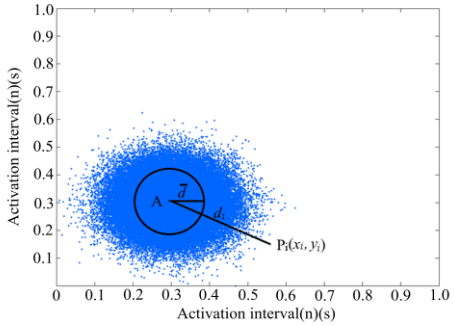

Figure 2. Schematic diagram associated with the ER value calculation. Point A was the geometric centre; $\bar{d}$ was the average distance; $\overline{AI}$ was the average activation interval; ER was the final evaluating index (ER = $\bar{d} / \overline{AI}$).

A. Dominant Frequency Distribution during AF

In Fig.3-a, we presented the mean DFs of different parts in atria. Please refer to Fig.1 for the abbreviation of various parts. DFs of each part were normalized to the ALA DF and the ratio was shown in Fig.4-a. AEG from the ALA had the highest activation rate, with a DF of 14.60Hz while AEG from the PRA had the lowest activation rate, with a DF of 6.51Hz. For both atria, the DFs of anterior part were higher than that of posterior one. For the right atrium, there was an obvious anterior-posterior gradient of DFs (P<0.005). The difference between the mean ARA and PRA DFs was 6.39Hz. For the four PV roots, DFs of the left PV were a bit higher than that of the right one. No inferior-superior gradient of DFs exist in the roots of PVs. However, there was a gradient between the atria and the roots of PVs (P<0.01).

B. Equivalent Radius Distribution during AF

In Fig.3-b, we presented the mean ERs of different parts in atria. ERs of each part were normalized to the ARA ER and the ratio was shown in Fig.4-b. The variability of activation rate of AEG from the ARA was the largest, with an ER of 0.459 while the variability of the LSPV was the smallest, with an ER of 0.226. The variability of activation rate in right atrium was larger than that in left atrium both anterior and posterior ERs. For the four PV roots, ERs were close to each other and a gradient exists between the atria and the roots of PVs (P<0.01).

IV. Discussion

The Fourier transform reveals that continuous signals can be decomposed into a sum of weighted sinusoidal functions. Frequency with greater weight has greater influence on the rhythm of the signal. Three 4-second-long AEGs chosen from ARA, ALA and RSPV were demonstrated in Fig.5 with their corresponding FFT. AEG from ARA has both a higher DF and a larger ER; AEG from ALA has a higher DF while a smaller

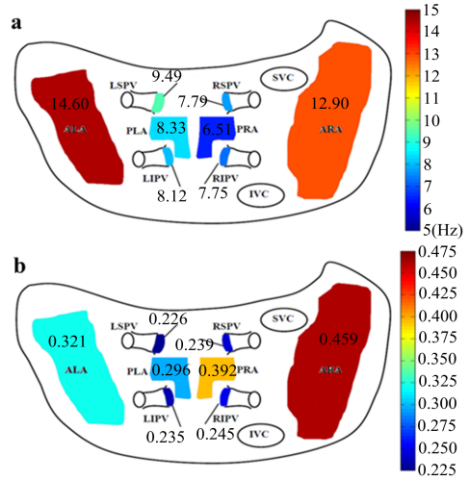

Figure 3. DF and ER distribution in atria and roots of PVs during AF. a, DF maps of epcardial surfaces of ALA, ARA, PLA, PRA and four roots of PVs. Areas of frequency maps indicated mapping field. b, ER maps of epicardial surfaces of the same parts as DF maps.

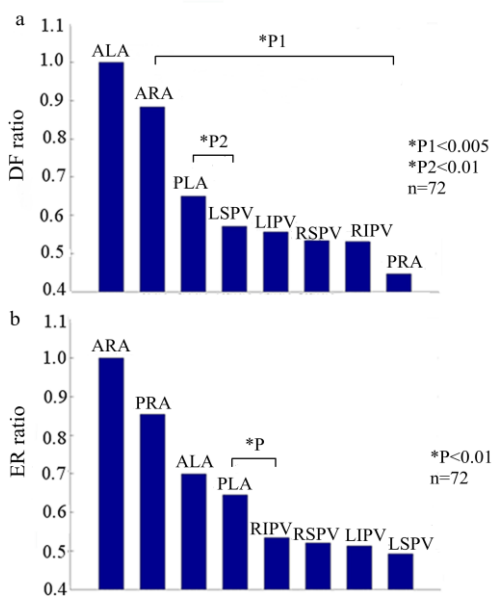

Figure 4. Gradients of activation rate and activation rate variability. a, Gradients of DF distribution. DFs was normalized to ALA DF at different locations and displayed in descending order. b, Gradients of ER distribution. ERs was normalized to ARA ER and displayed in descending order.

ER; AEG from RSPV has both a lower DF and a smaller ER.

As shown in Fig.5, the DF of ARA was 13.01Hz. However, apart from the maximum frequency, there were another two secondary large frequencies (7.93Hz and 14.12Hz) whose magnitude weight was greater than 0.8 in the FFT spectrum. Under the control of at least three frequencies, the activation rate variability of ARA signal was hard to be small. As shown in Fig.3-b, the ER of ARA was the largest one among the various parts of atria. For AEGs of ALA and RSPV, although they had different DF values, only one major frequency exist in their FFT spectrum. Single regular rhythm led to a smaller variability of activation rate. Hence, the ERs of these two parts were smaller than that of ARA as shown in Fig.3-b. Higher DF reflects more rapid activity of AEG while smaller ER reflects more regular activity of AEG. A combination of these two methods can provide more complete information about the activity of AEG.

Sites with high DFs have been guiding targets in current radio frequency ablation surgery [5, 6, 8]. However, Berenfeld *et al* observed multiple DF sites in a given individual, and although ablation at each site resulted in the slowing of the AF process, termination was observed at other sites in addition to the maximal DF site [6]. This situation may be related to signals with multi-rhythm. Only one frequency was regarded as DF while other greatly weighted frequencies were neglected. Taking the activation rate variability into consideration may make up for the shortfall. LP, as a common method to analyze the ECG HRV, may be appropriate for analyzing activation rate variability of AEG. A combination of DF and LP methods may provide a more comprehensive understanding of the electrophysiology mechanism associated with AF.

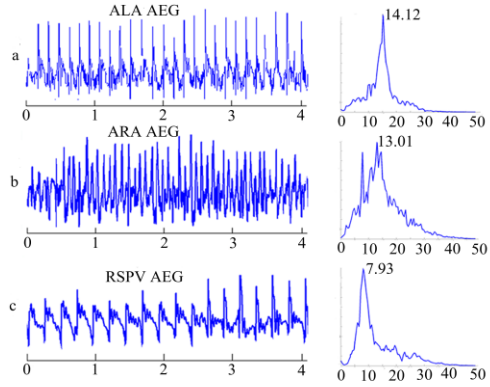

Figure 5. AEG from (a)ALA, (b)ARA and (c)RSPV with their corresponding FFT. AEG from ARA was a multi-rhythm signal, for its magnitude spectrum had another two secondary large frequencies except the maximum one (14.12Hz). AEG from ALA and RSPV were single rhythm signal with only one frequency of large weight.

V. Conclusion

DF is an effective tool to estimate activation rate of AF signals while LP is appropriate to evaluate the activation rate variability of AF signals. There are gradients of both activation rate and activation rate variability in the atria and the roots of PVs during AF. A combination of these two methods provides more complete information about the activity of AF signals.

References

[1] G. K. Moe, "On the multiple wavelet hypothesis of atrial fibrillation," *Arch Int Pharmacodyn Ther*, vol.140, pp.183-188. 1962.

[2] M. A. Allessie, W. Lammers and Bonke F, et al. "Experimental evaluation of Moe's multiple wavelet hypothesis of atrial fibrillation," in *Cardiac Arrhythmias*, Grune & Stratton. New York: 1985, pp.265-275.

[3] A. C. Skanes, R. Mandapati and O. Berenfeld, et al. "Spatiotemporal periodicity during atrial fibrillation in the isolated sheep heart," *Circulation,* vol.12-98, pp.1236-1248, Sep.1998.

[4] M. Mansour, R. Mandapati and O. Berenfeld, et al. "Left-to-right gradient of atrial frequencies during acute atrial fibrillation in the isolated sheep heart," *Circulation,* vol.21-103, pp.2631-2636, May.2001.

[5] O. Berenfeld, A. V. Zaitsev and S. F. Mironov, et al. "Frequency-dependent breakdown of wave propagation into fibrillatory conduction across the pectinate muscle network in the isolated sheep right atrium," *Circulation*, vol.11-90, pp.1173-1180, Jun.2002.

[6] C. Jose, I. Enrique and C. Juan, et al. "A new treatment for atrial fibrillation based on spectral analysis to guide the catheter RF-ablation," *Europace*, vol.6-6, pp.590-601, Nov.2004.

[7] P. Sanders, O. Berenfeld and M. Hocini, et al. "Spectral analysis identifies sites of high-frequency activity maintaining atrial fibrillation in humans," *Circulation*, vol.6-112, pp.789-797, Aug.2005.

[8] Y. Lin, C. Tai and T. Kao, et al. "Frequency analysis in different types of paroxysmal atrial fibrillation," *Journal of the American College of Cardiology*, vol.7-47, pp.1401-1407, Apr.2006.

[9] N. G. Jason and J. G. Jeffery, "Understanding and interpreting dominant frequency analysis of AF electrograms," *Journal of Cardiovascular Electrophysiology*, vol.18, pp.680-685, June.2007.

[10] H. D. Esperer, H. C. Esperer and J. B. Chernyak, "Risk stratification in advanced heart failure using Lorenz plot indies of heart rate variability," *IEEE , Computers in Cardiology*, pp.209-212. 2004.

[11] T. Zhou, D. Lin and C. Yang, et al. "Analysis of epicardial mapping electrogram of sustained atrial fibrillation based on Shannon entropy," in *2009 Conf. Proc. IEEE, Eng Med Biol Soc*, pp.3470-3472.

[12] E. C. Ifeachor, *Digital signal processing: A Practical Approach*. Beijing Publishing House of Electronics Industry, 2003, pp.647.

[13] L. Sun, L. Liu and Y. Wang, et al. “An adaptive filtering algorithm applied to inhibit the interference from the ventricular during atrial epicardial mapping experiment,” *Chinese Journal of Medical Instrumentation*, vol.35, pp.243-245. 2011.

[14] J. Pan and W. J. Tompking, “A real-time QRS detection algorithm,” *IEEE Biomedical Engineering*, vol.32, pp.230-236, Mar.1985.

[15] G. W. Botteron and J. M. Smith, “Quantitative assessment of the spatial organization of atrial fibrillation in the intact human heart,” *Circulation*, vol.3-93, pp.513-518, Feb.1996.

[16] T. H. Everett, L. C. Kok and R. H. Vaughn, et al. “Frequency domain algorithm for quantifying atrial fibrillation organization to increase defibrillation efficacy,” *IEEE Biomedical Engineering*, vol.48, pp.969-978. 2001.

[17] K. Tsuboi, A. Deguchi and H. Hagiwara, “Relationship between heart rate variability using Lorenz plot and sleep level,” in *2010 Conf. Proc. IEEE, Eng Med Biol Soc*, pp.5294-5297.

[18] M. Brennan, M. Palaniswami and P. Kamen. “New insights into the relationship between Poincare plot geometry and linear measures of heart rate variability,” in *2001 Proceedings of the 23rd Annual International Conference of the IEEE*, vol.1, pp.526-529.

[19] P. Strumillo and J. Ruta. “Poincare mapping for detecting abnormal dynamics of cardiac repolarization,” *IEEE Engineering in Medicine and Biology Magazine*, vol.21, 2002, pp.62-65.

[20] F. Wen, H. Chen and M. Wei, et al. “Research on analyzing approach of mapping plots of heart rate variability based on the first order difference sequence,” *Space Medicine & Medical Engineering*, vol.22-1, pp. 39-43, Feb.2009.